Chapter 6

hBCAT interacts with the molecular chaperone PDI

6.1 – Introduction:

Optimal cellular function relies on the interplay of various repair and chaperone systems. Thioredoxin, glutaredoxin, and PDI are repair enzymes that constitute the thioredoxin superfamily, which together co-ordinate adaptive response to changes in the cellular redox environment (Appenzeller-Herzog and Ellgard, 2008; Nakamura, 2005). PDI is able to catalyse the refolding of proteins by the formation and breakage of disulphide bonds through thiol:disulphide exchange, this relies on the CXXC of PDI. Similar to PDI, the hBCAT proteins have a conserved CXXC motif, where the thiols can recycle between an intra-molecular disulphide bond (inactive) and the reduced dithiol (active) (Tu *et al.,* 2000; Yennawar *et al.,* 2006). Furthermore, our group has demonstrated that the hBCAT proteins catalyse the insertion of disulphide bonds into rdRNase-releasing active RNase, with the active cysteines playing a key role in this mechanism (El Hindy *et al.,* 2014). This shows a novel role for hBCAT, whereby it can function as a foldase.

Molecular chaperones, such as the heat shock proteins (particularly HSP70 and HSP90) and PDI, are up-regulated in response to cellular stress in neurodegenerative diseases where they are believed to play a neuroprotective role (Andreu *et al.,* 2012). This protective effect is, however, compromised in neurodegenerative pathologies, whereby S-nitrosylation of the reactive thiols (SNO-PDI) compromises its disulphide-isomerase and chaperone activity. Due to this loss of function, SNO-PDI has been associated with misfolded protein aggregates in AD, Parkinsons's disease, and Amyotrophic Lateral Sclerosis (reviewed in Conway and Harris, 2015). Since PDI, and its compromised activity, play a role in neurodegenerative pathogenesis, it is vital to fully understand its cellular interactions.

PDI is most prominently expressed in the ER, initially suggesting that an interaction with hBCAT, either in the cytosol or the mitochondria, is unlikely.

However, there are studies supporting expression in other cellular regions including the mitochondria, nucleus and cytosol (Wilkinson and Gilbert, 2004; Rigobello *et al.,* 2001; Turano *et al.,* 2002). Furthermore, confocal microscopy and electron microscopy work showed PDI co-localisation with the mitochondrial redox protein, Mia40, providing further evidence of mitochondrial localisation (El Hindy *et al.,* 2014). This work also demonstrated co-localisation between both hBCAT isoforms and PDI, although the co-localisation with hBCATm (Mx 0.675) was stronger than with hBCATc (0.29) (El Hindy *et al.,* 2014).

As hBCAT has been observed occupying the same cellular space as PDI, this chapter aims to investigate if there is a direct binding interaction *in vitro*. Using both cell models and human brain homogenates, a co-immunoprecipitation method with Western blot analysis was optimised to this end. Due to the significant up-regulation of the hBCAT proteins in AD, their isomerase activity and interaction with PDI may play a crucial role in mediating the difference between correct protein folding and aggregate formation resulting in neurodegenerative pathology.

6.2 – Specific aims:

- **Specific aim 1:** Optimise an immunoprecipitation method for analysing protein-protein binding partners of hBCAT.
- **Specific aim 2:** Demonstrate hBCATm binding to PDI *in vitro* using co-immunoprecipitation and western blot analysis.
- **Specific aim 3:** Establish a method for overexpression of tagged-hBCAT to allow for pull-down analysis.

6.3 – Results:

The hBCAT proteins have been shown to play a role in protein folding (El Hindy *et al.,* 2014). In the context of AD, their role in mis-folding and subsequently autophagy is of significant interest. Previous research showing hBCAT and PDI co-localising suggests an interaction between the two proteins, possibly acting as a chaperone and facilitating correct protein folding. This potential interaction will be investigated further here through the use of immunoprecipitation analysis.

6.3.1 – Epitope availability in hBCAT under native conditions.

In order to carry out successful immunoprecipitation analysis, the primary antibodies used need to have an epitope that is not buried within the 3D structure of the *in vivo* protein conformation. Western blot analysis using native conditions would certify this, but first it was important to establish that the hBCAT and PDI proteins migrate appropriately through native PAGE to enable detection with antibodies. hBCATc, hBCATm, IMR-32 cell lysate, and protein ladder were loaded onto a 12% native PAGE gel. The gel was stained with GelCode Blue stain reagent and imaged on a gel doc (Figure 6.3.1). The molecular weight protein ladder (L1) failed to separate due to the native conditions used, but the hBCAT proteins (L2-7) and IMR-32 cell lysate (L8) have all progressed through the gel. This migration meant that it was possible to carry out a western blot on the non-denatured proteins.

To confirm that the epitopes for hBCATc, hBCATm and PDI antibodies are not buried within the *in vivo* conformational structures of the proteins within cells, western blot analysis was carried out on IMR-32 cell lysates and pure proteins separated by native PAGE (Figure 6.3.2). The hBCAT proteins did not migrate particularly far on the 12% gel previously used (Figure 6.3.1); therefore an 8% native PAGE gel was used to ensure sufficient migration of larger complexes. The

hBCATc, hBCATm and PDI antibody probes respectively show that a band has been detected in the IMR-32 cell lysates that is comparable to the pure protein lane (Figure 6.3.2). This validates that the primary antibodies used will be able to detect and bind their corresponding protein *in vivo* and therefore be suitable for use in immunoprecipitation experiments. Although there is only one band observed in the pure protein lanes, in the cell lysate lanes there are other forms of the protein present. In particular at positions a-c and e, proteins at this higher weight suggest either multimers or binding interactions with other proteins. The bands at positions d, f and g are potentially either splice variants of the specific protein, monomers, or differences in conformational structure present in IMR-32 cells. hBCATc migrated to a much lower point than hBCATm, despite both proteins having similar molecular weights, thus hBCATc in cells must have a significantly varying charge and hydrodynamic size causing it to migrate further (Figure 6.3.2). The detection of specific protein bands for hBCATc, hBCATm and PDI certifies that the epitopes for these antibodies are available for detection in their native forms.

6.3.2 - Western blot detection for PDI complexed with hBCATm in IMR-32 cell lysates.

Once epitope availability was established, the ability of hBCATm to bind to PDI was investigated using imunoprecipitation (IP) with antibodies specific for hBCATm. Western blot analysis, using an 8% SDS-PAGE, demonstrated that PDI was specifically isolated with hBCATm (Figure 6.3.3). The pure PDI band observed at 57 KDa demonstrates the validity of the PDI antibody and that PDI is highly expressed in these cells in both the cell lysates and supernatants. The presence of this PDI band in the experimental IP (L5) and not the IgG control IP (L2) demonstrates that PDI interacts with hBCATm in neuronal cells and that IgG does not interfere with the interaction. Additionally, the two bands at around 53 KDa (H) and 23 KDa (L) present in the control IP (L2) and the experimental IP (L5) are due

to the IgG heavy (53 KDa) and light (23.25 KDa) chain fragments. These are fragments from the primary antibodies bound to the protein G agarose beads that have been eluted and detected by the secondary antibody. The use of the mouse conformation anti-rabbit IgG conformation specific HRP antibody was intended to prevent this problem as the heavy chain fragment is particularly close to the expected PDI band at 57 KDa and could thus obscure its detection.

To optimise further, protein G mag sepharose beads were used as opposed to protein G agarose beads because they are non-adherent and thus eliminate smearing effects and aggregate formation. In addition to this, the protein samples were separated on a 6.5% SDS-PAGE in order to remove the IgG light chain band from the gel, and a mouse-raised anti-rabbit light chain specific antibody was used. Under these conditions a band for PDI was visualised at 57 KDa in the cell lysates, the pure PDI and importantly the experimental IP (Figure 6.3.4). The absence of a band in the control IP samples confirms that the proteins eluted are specifically hBCATm and that there is very little unspecific binding to the beads. The band in the experimental IP sample demonstrates that PDI was co-purified with hBCATm demonstrating that hBCATm directly binds to PDI in neuronal cells. Compared to the previous Western blot (Figure 6.3.3), there was significantly less smearing and a better separation between the PDI band and the IgG heavy chain (H) resulting in a clearer band for the experimental IP (Figure 6.3.4).

6.3.3 - Western blot detection for PDI complexed with hBCATm in temporal brain homogenates.

Temporal brain homogenates (800 µg) were incubated overnight with protein G mag sepharose bound to mouse raised anti-hBCATm. The eluted immunoprecipitated proteins, brain homogenates and pure PDI samples were seperated on a 6.5% SDS-PAGE gel and analysed by Western blot. A band for PDI was visualised at 57 KDa in the brain homogenates, the pure PDI and importantly

the experimental IP. The bands in the pure PDI and brain homogenate samples validate the anti-PDI antibody and also show that there is PDI present in the temporal region of this patients' brain. The absence of a band in the control IP samples confirms that the proteins eluted are specifically hBCATm and that there is very little unspecific binding to the beads. The band in the specific IP sample demonstrates that PDI was co-purified with hBCATm suggesting that hBCATm directly binds to PDI in the human brain (Figure 6.3.5). As observed in previous results (Figure 6.3.4), when a secondary HRP antibody is used for the same species that the antibody bound to the beads is from then the IgG heavy and light chain fragments will be detected. In the experimental IP, which used the mouse-raised anti-hBCATm, a band around 53 KDa corresponds to the IgG heavy chain.

Through optimising the immunoprecipitation method it has been clearly demonstrated that when hBCATm is immunopreciptated from both neuronal cell lysates and human brain homogenates, western blot analysis shows the presence of PDI. Therefore, hBCATm interacts with PDI in both a neuronal cell line and the human brain. To further validate these results, the use of a protein tag was developed as this provides an alternative method of binding hBCATm to beads without the use of an hBCATm antibody.

6.3.4 - hBCATm-His purification.

In order to assess whether overexpression of hBCATm with a 6X His tag would increase the amount of PDI immunoprecipitated from neuronal cells, a preliminary experiment was conducted using hBCATm with a 6X His tag overexpressed and purified from *E.coli*. The elution of purified hBCATm-His after ion exchange chromatography is shown in Figure 6.3.6a. The purity of the hBCATm-His was assessed by SDS-PAGE analysis (Figure 6.3.6b). The single band at 43 KDa in lanes 8 and 9 suggests high purity of the M1 fraction. Additionally, throughout the sequential washes (L2-L6) the purity of the hBCATm-

His can be seen to increase demonstrating that the hBCATm-His has not been lost at earlier steps in the purification but has been successfully purified and eluted into buffer D (L6). The hBCATm-His can be seen to have been successfully transferred into Mono Q buffer A (L7), purified by ion exchange (L8) and dialysed into stable buffer (L9) without any significant loss of the protein or its purity.

6.3.5 - Precipitation of IMR-32 cell lysate with hBCATm-His bound to Ni Sepharose™ beads.

Purified hBCATm-His was subsequently bound to Ni Sepharose™ beads and incubated overnight with IMR-32 cell lysates. The bound proteins were eluted with 767 mM imidazole and separated by SDS-PAGE. As demonstrated in Figure 6.3.7, the increase in the quantity of eluted hBCATm-His can be seen (L2-5) showing that the Ni sepharose beads are binding the tagged protein. Additionally, there are a number of other protein bands present and so the Ni sepharose beads are not specifically just binding the hBCATm-His but also other proteins from the cell lysate either due to the beads themselves or binding interactions of hBCATm. The Ni sepharose beads plus cell lysate (L7), without any hBCATm-His bound, show a number of bands representing cellular proteins that bind to the beads without the presence of hBCATm. Western blot analysis comparing these samples will show if there are proteins not present in the beads without hBCATm-His but are there due to an interaction with hBCATm.

6.3.6 - Western blot detection of PDI from precipitated hBCATm-His bound to Ni Sepharose™ beads and incubated with IMR-32 cell lysate.

To determine if hBCATm-His interacts with PDI *in vivo*, the precipitated proteins bound to hBCATm-His were eluted and separated by SDS-PAGE and transferred to a PVDF membrane. The membrane was probed for PDI and bands were observed in all lanes with the exception of the sequential washes (L9-11). The

band in the IMR-32 cell lysate (L1) and the pure PDI (L6) validate the antibody and also demonstrate that there is PDI present in IMR-32 cell lysate. The band in the flow through (L8) suggests that not all of the PDI in the IMR-32 cell lysate has bound to the beads. There is a band present in the beads bound to hBCATm-His samples (L2-L5), however, using this method it cannot be concluded that PDI is binding to hBCATm, due to the band in the bead only (L7) lane (Figure 6.3.8). This suggests that PDI binds to the Ni sepharose beads non-specifically irrespective of hBCATm, indicating that a different form of capture should be used to precipitate hBCATm-His.

In summary, using a pull-down method with His-tagged hBCATm did not clearly demonstrate a binding interaction with PDI. Therefore, the optimised immunoprecipitation method provided the best quality of results in regards to examining the protein interactions of hBCATm. This method can now be expanded to examine interactions with other potential binding partners in future work.

6.3.7 - Western blot analysis of IMR-32 cell lysate transfected with hBCATm-His and bound to His Mag Sepharose Ni.

Confluent IMR-32 cells were transfected with hBCATm-His expression vector DNA using jetPRIME® transfection reagent and incubated at 37°C for 9, 24, 32 and 48 hours. The cell lysates were extracted and analysed using western blot analysis. From the density of the bands observed in Figure 6.3.9 A it can be seen that the expression of hBCATm-His increases over the selected time periods (L2-L5), where a time-dependent increase in protein expression is observed. A 30 minute pull-down was carried out using 75 µL of His Mag Sepharose Ni and 150 µL of the cell lysate from the 48 hour overexpression of hBCATm-His alongside a control using the 48 hour overexpression of Gus. The eluted precipitation proteins were also analysed using western blot analysis (L8+L9) in Figure 6.3.9 A and B. The hBCATm probe (A) produced a single band in the overexpressed pull-down

(L8) and not in the Gus overexpression pull-down (L9). This demonstrates that the His tag on the synthesised hBCATm successfully binds to the His Mag Sepharose Ni beads and that cellular hBCATm only specifically binds to the antibody. In the PDI probe (B) there are bands observed in both pull-down lanes (L8+9) which suggests that PDI non-specifically interacts with the His Mag Sepharose Ni beads, despite not having a 6X His tag and independent of any potential protein interactions with hBCATm. To investigate this further, a low concentration of imidazole was used to attempt to displace non-specific binding from nickel co-ordination in combination with varying amounts of total protein in the incubation step.

6.3.8 - Western blot analysis of overexpressed hBCATm-His in IMR-32 cells pulled-down with His Mag Sepharose Ni beads.

Once IMR-32 cells had been transfected with hBCATm-His for 48 hours, a pull-down experiment was carried out with 500 µg and 800 µg of cell lysate in 30 mM imidazole IP buffer, and 500 µg of cell lysate in 20 mM imidazole IP buffer (Figure 6.3.10). This was to investigate whether using imidazole in the IP buffer would reduce non-specific binding, along with varying the amount of total cell lysate in relation to the 60 µL of His Mag Sepharose Ni beads. As confirmation of successful transfection, the overexpressed hBCATm can be seen clearly in the non-transfected (L1) and transfected (L2) cell lysates when probed for hBCATm (B) in regards to a significant increase in density. Despite hBCATm being clearly detected in both of the cell lysates there are no observable bands in either of the transfected pull-downs (L3-5) or the non-transfected control (L6-8). This means that the hBCATm-His is not binding to the His Mag Sepharose Ni beads at the amounts of protein used and also the concentration of imidazole. In the PDI probe (A) there are bands observed in both the transfected and non-transfected pull-downs supporting

the previous findings that PDI is binding preferentially to the beads independent of hBCATm-His interactions.

6.3.9 – Western blot analysis of immunoprecipitated overexpressed hBCATm-His in IMR-32 cells.

Due to the unsuccessful pull-downs using the 6X His tag of hBCATm-His it was decided to revert to an immunoprecipitation to see if the overexpression of hBCATm, regardless of the 6X His tag, would increase the previously observed interaction with PDI. After binding 1 µg anti-hBCATm to protein G Mag Sepharose beads for 1 hour, 800 µg of cell lysate from IMR-32 cells transfected with hBCATm-His was incubated with the beads overnight. The eluted immunoprecipitated proteins, cell lysates and pure PDI samples were separated by SDS-PAGE gel and transferred onto a PVDF membrane for western blot analysis. Using chemiluminescent substrate a band for PDI was visualised at 57 KDa in the cell lysates (L1-2), the pure PDI (L5) and importantly the precipitated proteins (L3-4) (Figure 6.3.11). The bands in the pure PDI and cell lysate samples validate the anti-PDI antibody and also show that there is PDI present in the IMR-32 cells. The absence of a band in the control IP samples (L6-7) confirms that the proteins eluted are specifically hBCATm and that there is very little unspecific binding to the beads. The band in the specific IP sample demonstrates that PDI was co-purified with hBCATm supporting previous results demonstrating that hBCATm directly binds to PDI in neuronal cells.

6.3.10 – Site-directed mutagenesis of hBCATm entry vector.

Due to the N-terminal 6 X His tag not resulting in specific pull-downs of hBCATm, a Gateway® pcDNA™-DEST47 vector was purchased from Life Technologies. This vector contains a C-terminal GFP tag, but in order to re-combine the hBCATm entry vector with this destination vector, site-directed

mutagenesis was required to remove the stop codon after the hBCATm gene (bases 1205-8). If this stop codon was not removed, the transfected final expression vector would be likely to produce two populations of hBCATm, one with the C-terminal GFP tag and another without it, due to the DNA polymerase recognising the stop codon after the hBCATm gene. Site-directed mutagenesis was carried out using 50 ng and 100 ng of template DNA (hBCATm entry vector) as per the manufacturer's guidelines using resynthesized complementary oligonucleotides for the mutation of the hBCATm stop codon. The primers designed for this mutation changed the TGA stop codon to a GGC codon which codes for alanine, a non-polar amino acid. After the mutagenesis synthesis reaction, the methylated and hemimethylated (non-mutant) plasmids were digested with Dpn I. This endonuclease digests the parental DNA template and thus selects the mutation-containing synthesised DNA. A control reaction was carried out using a pWhitescript plasmid in order to assess the efficiency of the mutagenesis kit. Post digestion, the samples were separated on a 0.8% agarose gel (Figure 6.3.12). A single band at 4.5 kb in lane C represents the pWhitescript control plasmid and the bands resolved at approximately 4 kb are the mutated hBCATm entry vector (A+B). The absence of additional bands, or any bands in the negative control (D), suggests that there is no sample contamination.

After the Dpn I digestion, the mutant plasmids and the pWhitescript control were transformed into XL 10-Gold ultracompetent *E.coli* as instructed by the manufacturer's instructions. The transformation efficiency was calculated from the pUC18 plate to be 8.4 x 10^8 CFU/µg (>10^9 CFU/µg expected) and the mutagenesis efficiency was calculated from the pWhitescript plate to be 98% (> 85% expected). The hBCATm entry plasmid mutant colonies were selected from these plates, grown overnight and purified by mini-prep. To confirm the mutation of the stop codon in the hBCATm gene, the purified hBCATm mutant vectors were sent to Eurofins MWG Operon at a concentration of 100 ng/µL for sequencing analysis. Figure

6.3.13 highlights the difference between the non-mutated hBCATm entry vector (A) and the mutated hBCATm entry vector (B). The area highlighted in the red boxes clearly shows the original TGA stop codon and the mutated GGC alanine codon confirming successful site-directed mutagenesis. To check that the mutated sequence was still in-frame, sequence alignment was carried out using NCBI BLAST® (C). The upper sequence is the non-mutated hBCATm entry vector and the lower sequence is the mutated hBCATm entry vector. The two sequences are still aligned with the exception of the highlighted mutated region (C), confirming that the mutagenesis was successfully site specific.

6.3.11 – Creating the hBCATm-GFP expression vector.

The mutated hBCATm entry vector was recombined into a Gateway® pcDNA™-DEST47 vector for human cell expression using the LR Clonase® II enzyme mix. The completed reaction was then transformed into Library Efficiency® DH5α™ cells and spread onto LB plates. In order to calculate the transformation efficiency, blue/white colonies were visualised after 24 hours for the pUC19 plates, where white colonies were positive transformants containing the pcDNA™DEST47 vector along with the mutated hBCATm gene. The transformation efficiency was calculated to be 6.36×10^7 CFU/µg. The subsequent hBCATm-GFP expression vector was purified by mini-prep, from which 1 µg was loaded onto a 0.8% agarose gel in order to assess sample purity (Figure 6.3.14). In lanes A, C and E there is a band at approximately 4 kb which is the supercoiled expression vector, approximately half of the actual size of the expression vector which is shown faintly at 8 kb. Restriction digest of the expression vector was used to confirm that the vector contained the mutated hBCATm gene along with the specific restriction sites. This is demonstrated in lanes B, D and F by the lower band at 1.2 kb which is the hBCATm gene, and the remaining linear plasmid at 6.8 kb. The absence of any additional bands suggests that there is no sample contamination. The expression

vector is now ready for transfection into IMR-32 cells to carry out pull-down and cell imaging experiments using the C-terminal GFP tag.

6.4 – Discussion:

The accumulation of misfolded proteins is a key characteristic of neurodegenerative diseases (Nakamura *et al.,* 2012). There is evidence to suggest that misfolded proteins are produced in healthy cells, but cellular mechanisms prevent their accumulation. These mechanisms include molecular chaperones that promote correct protein folding and reduce toxic aggregation, the ubiquitin protease system that targets misfolded proteins for degradation, and lysosomal autophagic degradation for removal of large protein complexes (Nakamura and Lipton, 2011). Furthermore, all of these processes are sensitive to oxidative stress which is strongly linked to AD by the damaging effects of free radicals (Christen, 2000). However, the mechanisms which link all of these processes in the context of AD are still not clearly defined.

Both the cytosolic and the mitochondrial hBCAT isoforms have demonstrated oxidase and thiol isomerase activity in the refolding of RNase A, dependent on the redox environment (El Hindy *et al.,* 2014). Protein folding mainly occurs in the ER, through PDI-mediated reactions, but can also occur in the mitochondria through the oxidoreductase Mia40 (Hatahet and Ruddock, 2009; Chacinska *et al.,* 2004). Studies using confocal and electron microscopy have shown co-localisation of hBCATm with both PDI and Mia40 in the mitochondria (El Hindy *et al.,* 2014). However, it is not known whether or not there is a specific interaction between hBCATm with PDI and Mia40 for a role in preventing misfolding of proteins.

6.4.1 – Native analysis of hBCATc, hBCATm and PDI.

The hBCATc, hBCATm and PDI proteins were analysed in their native form as part of the immunoprecipitation method development. Electrophoretic analysis of intact, enzymatically active protein complexes is only possible under non-denaturing

conditions, in contrast to SDS-PAGE (Laemmli, 1970). The movement of proteins in native PAGE is dependent on both the intrinsic charge on the protein at the pH of the running buffer and also its hydrodynamic size. Hydrophobic proteins are known to aggregate artificially during native electrophoresis (Lin *et al.,* 1999). Potential issues of using non-denaturing conditions are that dimer formation could result in the complex being too large in size to progress through the gel or that proteins in their non-denatured conformation lack the significant negative charge required for adequate electrophoresis.

The hBCAT proteins are homodimers with molecular masses ranging between 41 to 46 KDa. The molecular mass of the hBCATm subunit is 42.3 KDa, with each monomer consisting of 365 amino acid residues with one pyridoxal phosphate (PLP) as cofactor (Davoodi *et al.,* 1998; Yennawar *et al.,* 2001). The hBCATc subunit has a molecular mass of 42.8 KDa, with each monomer consisting of 385 amino acid residues and requires one PLP as cofactor (Davoodi *et al.,* 1998). Despite the 58% homology between the two amino acid sequences (Goto *et al.,* 2005), under native conditions hBCATc migrates significantly further in comparison to hBCATm (Figure 6.3.1 and Figure 6.3.2). This suggests that either the hydrodynamic size of hBCATc differs significantly to that of hBCATm, or the intrinsic negative charge of hBCATc is greater than that of hBCATm.

In addition to the two key mammalian isoforms identified, the cytosolic and mitochondrial, there are other known splice variants that are homologous to hBCATm, including a novel alternative splice variant found in placental tissue and a splice variant that acts as a co-repressor of thyroid hormone nuclear receptors (Lin *et al.,* 2001; Than *et al.,* 2001). Native Western blot (Figure 6.3.2) demonstrated that there are numerous conformations of PDI, hBCATc and hBCATm in neuronal cells. This result provided several specific protein bands located both above and below the pure protein band for all three proteins. The bands that are above are

most likely to be multimers or protein-protein interactions, thus increasing the hydrodynamic size of the protein complex. The bands that are below are potentially the monomeric forms of the proteins or perhaps novel neuronal splice variants. These findings present avenues for further exploration into potential novel protein-protein interactions and neuronal forms of these proteins. In future work, use of a molecular weight marker specifically for native gels would aid in identification of the protein bands which could also be analysed by mass spectrometry.

6.4.2 – hBCATm interaction with PDI.

Co-immunoprecipitation experiments using neuronal cell cultures (Figure 6.3.4), established that immunoprecipitated hBCATm has selectively isolated PDI demonstrating direct binding. Moreover, this result has been replicated in the human brain from a co-immunoprecipitation using human brain homogenate (Figure 6.3.5). These findings suggest a physiologically relevant role to the interaction between hBCATm and PDI, supporting a potential role for hBCATm in acting as a protein chaperone during folding.

PDI has been reported to interact with a variety of redox and non-redox sensitive proteins (Laurindo *et al.,* 2012). In particular, other proteins that bind with PDI and are involved in facilitating correct protein folding include FAD-binding ER oxidoreductin 1 (Ero-1), peroxiredoxin 4, and the G-protein coupled receptors Grp78 and Grp94 (Zito *et al.,* 2010). Redox interactions have also been identified between hBCAT and neuronal proteins involved in G protein cell signalling, including β-tubulin, septin 4, kalirin RhoGEF, sodium channel type 10 α, and myosin 6 (Conway *et al.,* 2008). Given that both PDI and hBCAT have known redox associations, it is plausible that similar interactions are taking place.

The formation of new disulphide bonds by PDI is an oxidation reaction whereby the substrate nucleophilic cysteine attacks the PDI disulphide, forming a

mixed PDI-substrate disulphide. The substrate is then released oxidised after transferring reducing equivalents to PDI. This leaves PDI in a reduced form, i.e. an inactive conformation (Laurindo *et al.,* 2012). Therefore, the protein folding carried out by PDI is a synergistic effect, requiring other protein interactions to facilitate the regeneration of its active conformation.

The presence of Ero-1, a FAD-binding oxidase, has been suggested to be required for the catalytic activity of PDI (Gilady *et al.,* 2010). In human cells, Ero-1 α and Ero-1 β have been shown to mediate re-oxidation of PDI by transferring oxidative equivalents via their CXXCXXC active sites (Figure 5.1) (Sevier *et al.,* 2007). As hBCATm also has a redox-active CXXC motif, the interaction observed with PDI could be redox mediated. However, Ero-1 knock-out studies have shown very little physiological consequences causing debate as to whether Ero-1 is the primary donor of oxidising equivalents or perhaps other mechanisms substitute for its absence in these models (Zito *et al.,* 2010).

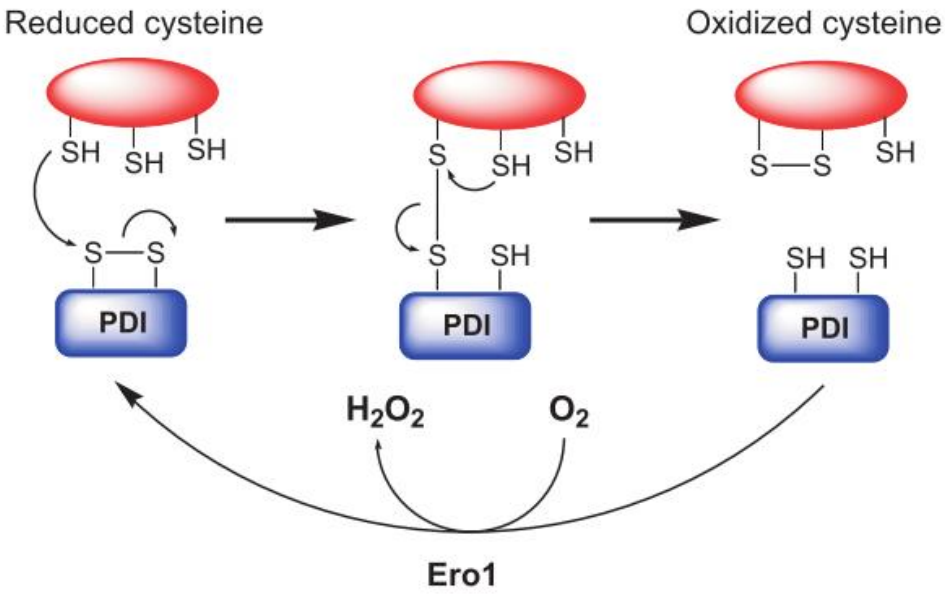

Figure 6.4.1 - Proposed chaperone role for Ero-1 in the oxidation and regeneration of PDI during protein folding. PDI oxidises substrate cysteine thiols to intramolecular disulphides for correct protein folding. To regenerate oxidised PDI, Ero-1 reduces O_2 to

H_2O_2 with simultaneous oxidation of PDI (Reproduced with permission from American Chemical Society) (Adapted from Forrester *et al.,* 2006).

The specific interaction of hBCATm with PDI demonstrated that transfection and pull-down analysis is a successful model that can be used to investigate hBCAT protein interactions with other redox partners, such as Mia40. The results presented here have revealed that hBCATm plays a role in protein folding as a molecular chaperone with PDI. The implications of these findings in the human brain are physiologically relevant and also important in developing understanding of the protein misfolding process, and consequently AD pathogenesis. Mia40 is another crucial oxidoreductase enzyme which is present in the mitochondria; therefore it will be interesting to investigate if hBCATm also associates with Mia40 as a molecular chaperone.

6.4.3 – An hBCATm tag for analysis of protein interactions.

The overexpression of hBCAT has been demonstrated and discussed in detail in Chapter 3. However, the use of protein tags to analyse the protein interactions of hBCAT can also be facilitated through the Gateway cloning system. There are numerous protein tags available, including His, GST, GFP and FLAG. The pDEST™26 vector used for recombination with hBCATm contained an N-terminal 6X His-tag for detection and purification using a metal-chelating resin such as Ni-NTA. Previous use of overexpressed hBCATm with an N-terminal 6X His-tag by Davoodi *et al.,* (1998), found that low levels of purification were due to the tag being buried. In 4 M urea the tertiary or quaternary structure of the protein was altered enough to facilitate binding of the His-tag, but the specific enzyme activity was compromised by 50% (Davoodi *et al.,* 1998). The overexpression and purification of hBCATm carried out by Davoodi *et al.,* (1998) was in *E.coli* and so it was hoped that the hBCATm protein folding may differ in humans to the extent that

the N-terminal tag would be exposed. Furthermore, use of urea was not suitable in this context of examining protein interactions between hBCATm and PDI.

The use of an N-terminal 6X His-tag with hBCATm for overexpression in IMR-32 cells did not result in successful pull-downs with His Mag Sepharose Ni beads (Figure 6.3.10). The magnetic beads used had a binding capacity of approximately 50 mg histidine-tagged protein/mL of medium. This high binding capacity should have resulted in a significant increase in concentration of the hBCATm-His from the cell lysate, but in Figure 6.3.10 there are no bands present in the pull-down lanes. These findings demonstrated that the His Mag Sepharose Ni beads were not pulling-down hBCATm-His. There are a number of possible reasons for this. One is that the cell lysates were only incubated with the beads for 30 minutes. Although 30 minutes at room temperature is the manufacturers recommend conditions, perhaps a longer binding time may result in a larger quantity of hBCATm-His binding. Another reason is a combination of two issues; the N-terminal 6X His-tag is partially buried, an issue previously found in *E.*coli (Davoodi *et al.,* 1998), and also the preferential binding of PDI. As shown in Figure 6.3.10 there are clear bands indicating that PDI is pulled-down by the His Mag Sepharose Ni beads. Upon analysis of the crystal structure of PDI (Figure 6.4.2), a large number of histidine residues are exposed. This quite likely resulted in PDI having a greater binding affinity to the beads compared to the partially buried 6X His-tag of hBCATm.

Another tag that was considered for use with hBCATm was the FLAG-tag. The FLAG-tag is a hydrophilic octapeptide (DYKDDDDK) that is based on antibody purification by M1 monoclonal antibody (mAb) and the last five amino acids are the recognition sequence for enterokinase protease (Arnau *et al.,* 2005). The tag can be doubled or tripled and has been reported to produce high purity proteins (Lichty *et al.,* 2005). A likely issue with using hBCAT proteins with a FLAG-tag is that as

the tag is so small it may easily become buried due to the conformation of either the N or C-terminus.

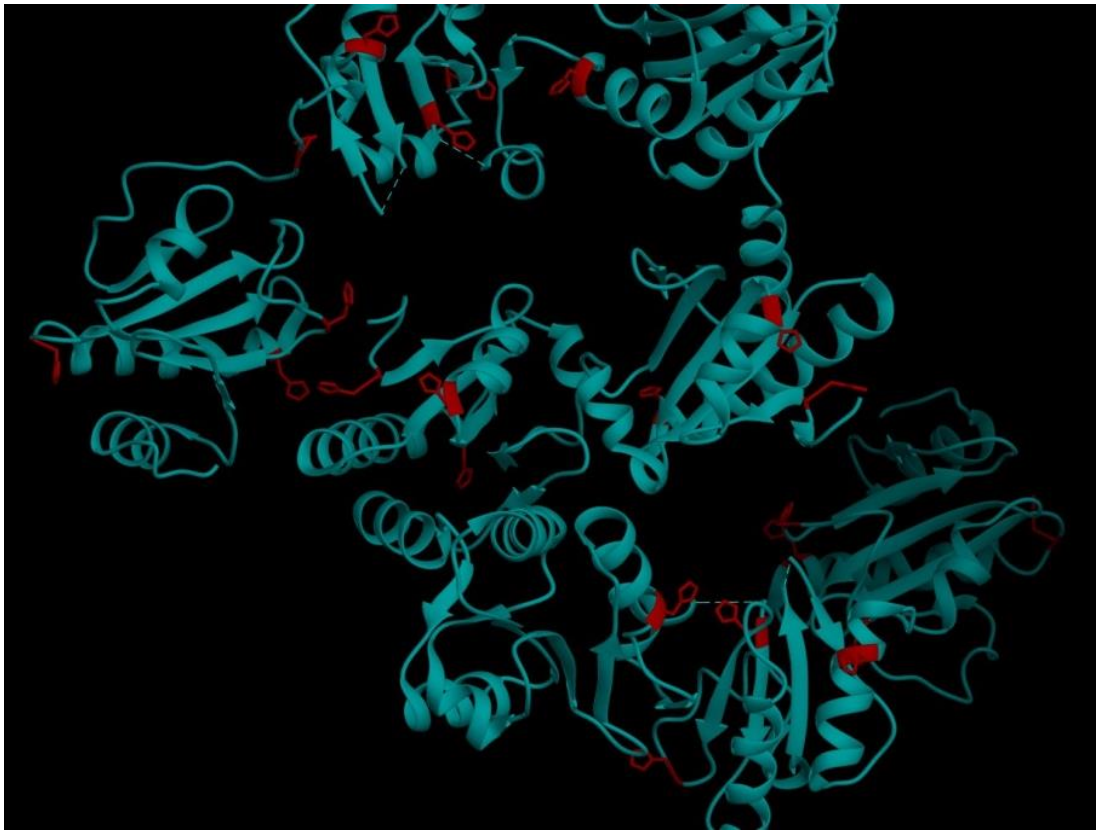

Figure 6.4.2 – Histidine residues of human PDI. The crystal structure of oxidized human PDI (Wang *et al.,* 2013) was analysed using Chimera 1.8. The large number of exposed histidine residues of PDI can be seen highlighted in red.

The green fluorescent protein (GFP), discovered nearly 40 years ago in the jellyfish *Aequorea victoria* and was first used as a molecular tag to track gene expression in 1994 (Shimomura *et al.,* 1962; Chalfie *et al.,* 1994). GFP fluorescence occurs due to aequorin interacting with Ca^{2+} ions which emits luminescence energy (488 nm). This luminescent energy is then transferred to GFP, which results in emission in the green wavelength at 509 nm (Morise *et al.,* 1974). Fluorescent proteins such as GFP are excellent tools for use as a protein marker in live-cell imaging to study subcellular distribution and dynamics (Muller-Taubenberger and Anderson, 2007). Furthermore, in studies investigating mTOR

signalling in autophagy, key proteins such as ATG13 have been tagged with GFP and successfully immunoprecipitated using protein G sepharose beads for complex analysis (Ganley *et al.,* 2009). The cycle 3 GFP used as a C-terminal tag in pcDNA™-DEST47 vector has spectral excitation and emission wavelengths identical to wild-type GFP, but contains four mutations to increase the brightness. Figure 6.3.14 shows the successful recombination of hBCATm into pcDNA™-DEST47 and is now ready for future experiments in analysing hBCATm interactions.

6.4.4 – Summary.

In summary, a specific interaction between hBCATm and PDI has been established through the use of immunoprecipitation analysis. This is a novel finding which supports previous work by our group, demonstrating hBCAT dithiol-disulfide isomerase activity and co-localisation between hBCAT and PDI (El Hindy *et al.,* 2014). The optimised method can also be used in future to examine novel protein interactions of hBCATm with other proteins such as Mia40, the other cellular protein key to protein folding. Furthermore, an overexpression model has been optimised for forthcoming analysis of hBCATm with a C-terminal GFP tag. This will allow live cell imaging to monitor hBCAT localisation over time, particularly upon cell treatment, to further investigate the role hBCAT plays in key cellular processes and protein misfolding responses.